Hindawi Publishing Corporation
Journal of Nanomaterials
Volume 2016, Article ID 2358276, 9 pages
http://dx.doi.org/10.1155/2016/2358276

Research Article

Inorganic Antiflaming Wood Caused by a TiO_2-Decorated ZnO Nanorod Arrays Coating Prepared by a Facile Hydrothermal Method

Hong Zhang,[1] Weigang Zhang,[1] Chunde Jin,[1] and Song Li[1,2]

[1]*School of Engineering, Zhejiang A&F University, Lin'an, China*
[2]*Key Laboratory of Wood Science and Technology, Lin'an, China*

Correspondence should be addressed to Song Li; li123song@163.com

Received 30 March 2016; Revised 8 June 2016; Accepted 31 August 2016

Academic Editor: Yogendra Mishra

Wood materials with antiflaming capability were successfully fabricated by depositing a TiO_2-decorated ZnO nanorod arrays (ZNAs) film on wood surface using a facile and one-pot hydrothermal method. The prepared specimens were characterized by scanning electron microscopy (SEM), energy dispersive X-ray analysis (EDXA), and powder X-ray diffraction (XRD). To explore the antiflaming properties, the combustion parameters of the wood treated by TiO_2-decorated ZNAs were measured using the cone calorimetry technique compared with the untreated wood. For treated wood, the burning duration was prolonged for 55 s; smoke production rate (SPR) and total smoke production (TSP) were obviously reduced, especially for the production of CO was almost zero. As a result, thin inorganic film of TiO_2-decorated ZNAs had desirable fire resistance, and one-pot hydrothermal method was a feasible method to fabricate nonflammable wood materials.

1. Introduction

Wood may be one of the most versatile materials in nature. It is renewable, sustainable, easily workable, aesthetically pleasing, and of excellent physical and mechanical properties [1–3]. For centuries, wood or wood-based products have been used in construction both structurally and decoratively. However, due to its natural combustibility, wood burns if exposed to severe fire conditions. When wood burns, it gives off light, heat, and gases including carbon dioxide, water vapour, and some toxic volatiles like carbon monoxide and oxides of nitrogen, which will lead to serious environmental pollution and human health safety problem [4–9]. Therefore, improving the fire performance of wood or wood-based products is becoming necessary and significative.

Since wood ignition and burning are surface processes, wood surface treatments may prevent ignition and burning and are considered as a potential and promising way to improve the fire performance [6, 10–15]. Fire retardants for wood surface treatments can be mainly divided into two groups named intumescent and nonintumescent coatings. Intumescent coatings are usually varnishes or paints while nonintumescent coatings are organic materials similar to those used in pressure impregnation [16–18]. But no matter intumescent or nonintumescent surface treatment, they eventually increase the production of wood smoke and toxic volatiles when wood fired. Therefore, how to efficiently hinder wood surface from fire and diminish wood smoke has attracted much attention in both scientific field and industrial regions [19–21]. Choosing appropriate nanomaterials is a possibility for developing an efficient and clear wood flame retardant because the synergistic effects resulting from the physical or chemical interactions between the nanomaterials and the wood substrate are able to produce such properties as improved thermal, mechanical, and dimensional stability [4, 6, 13, 22, 23].

Nano titanium dioxide (TiO_2) and zinc oxide (ZnO) species may be a favourable choice as a potential wood flame retardant in response to their merits of being nontoxic, high fire resistance, low cost, being environmentally friendly, and highly thermal stability [4, 24–28]. It is well known that ZnO is a direct bandgap semiconductor with an energy

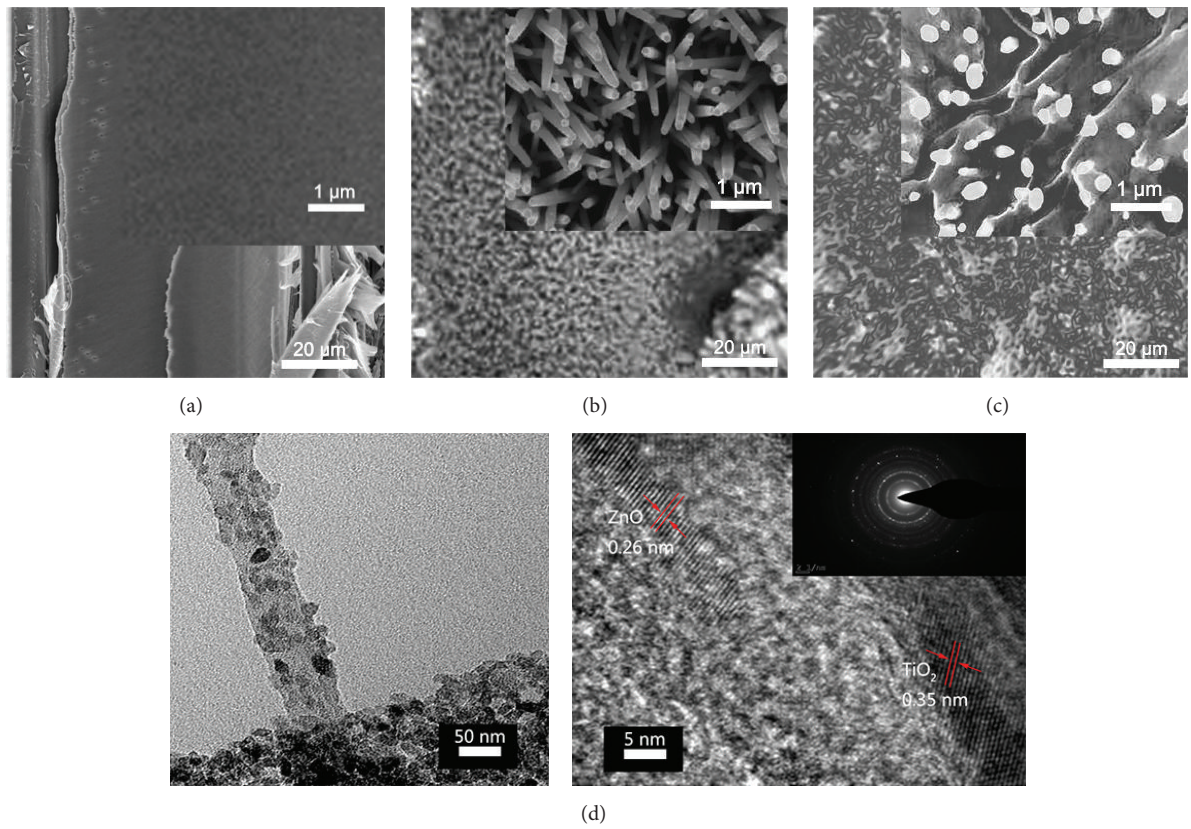

Figure 1: Surface SEM images of (a) untreated wood; (b) treated wood by ZnO nanorod arrays; and (c) treated wood by TiO_2-decorated ZnO nanorod arrays, respectively. The inset SEM images are the corresponding high magnification SEM images. (d) TEM image, HRTEM image, and SAED pattern of TiO_2-decorated ZnO nanorod arrays peeled off from the wood surface.

gap of 3.37 eV, while TiO_2 is an indirect bandgap with an energy gap of 3.0 eV (anatase) or 3.2 eV (rutile); ZnO or TiO_2 nanostructures are one of the most investigated materials for different nanotechnological applications [29–31]. Singla et al. [32] reported the optical properties of ZnO nanoparticles capped with different surfactants. However, at present, the nanomaterials coating for wood fire performance is only composed of monomeric inorganic materials such as TiO_2, SiO_2, and ZnO [33–39]. Though they exhibited improved fire performance, they cannot completely hinder wood from fire and diminish wood smoke production. Herein, we prepared inorganic antiflaming wood caused by a TiO_2-decorated ZnO nanorod arrays coating prepared by a facile hydrothermal method. The treated wood specimens showed a greatly improved antiflaming ability and almost no production of carbon monoxide. Furthermore, the heat release rate of the treated wood was also decreased.

2. Materials and Methods

2.1. Materials. All the reagents used in the experiments were of analytical grade (purchased from Shanghai Boyle chemical Co., Ltd.) and used without further purification. Wood specimens from the air-dried poplar lumber were cut into a size of 100 mm (longitudinal) × 100 mm (tangential) × 10 mm (radial).

2.2. Formation of ZnO Nanorod Arrays (ZNAs) on Wood Surface. In a typical process, ZNAs-coated wood specimens were achieved through the two following procedures. (1) Preparation of ZnO colloid and deposition onto the wood surface: 200 mL of 0.01 M alcoholic zinc acetate dehydrate solution was prepared and heated to 60°C under magnetic stir. Then, 104 mL 0.03 M alcoholic sodium hydroxide was dropwise added and stirred for 2 h at 60°C. Thus, a transparent and stable ZnO colloid was attained. The wood specimens were subsequently dipped into the ZnO colloid for 30 min, removed from the solution, and placed at room temperature for 6 h. After that, the obtained samples were dried at 105°C for another 3 h. This process was repeated for 15 times. The ZnO nanoseed-coated wood specimens were collected for the next hydrothermal synthesis. (2) Growth of ZNAs: 500 mL of 0.015 M aqueous solution of zinc nitrate hexahydrate and 500 mL of 0.015 M aqueous solution of hexamethylenetetramine were mixed together in a capped bottle. The above ZnO nanoseed-coated wood specimens were then placed into the solution. The bottle was sealed and placed into a water bath at 95°C for 12 h with moderate shaking. Finally, the ZNAs-coated wood specimens were removed from the solution, ultrasonically rinsed with deionized water for 30 minutes, and dried at 45°C for over 24 hours in vacuum. The surface morphology of ZNAs-coated wood was observed from SEM image shown in Figure 1(b).

2.3. Synthesis of Wood Treated by a TiO_2-Decorated ZNAs Coating. 10 mL tetrabutyl orthotita (TBOT) was firstly dissolved in 1000 mL anhydrous ethyl alcohol (EtOH) with magnetic stir for 30 minutes to form TiO_2 sol and transferred into a Teflon-lined stainless steel autoclave. ZNAs-coated wood specimens were subsequently placed into the above reaction solution. The autoclave was sealed and maintained at 150°C for 10 h and then cooled to room temperature naturally. Finally, the prepared samples were removed from the solution, ultrasonically rinsed with deionized water for 30 min, and dried at 45°C for over 24 h in vacuum. This process was repeated for 6 times. The surface morphology of wood treated by TiO_2-decroated ZNAs was observed from SEM image shown in Figure 1(c).

2.4. Characterizations. The surface morphologies of the specimens were observed by scanning electron microscopy (SEM, FEI, Quanta 200). The chemical compositions of the specimens were measured by energy dispersive X-ray analysis (EDXA, attached to the SEM). The crystalline structures of the specimens were identified by X-ray diffraction (XRD, Rigaku, D/MAX 2200) operating with Cu Kα radiation (λ = 1.5418 Å) at a scan rate (2θ) of 4°/min with the accelerating voltage of 40 kV and the applied current of 30 mA ranging from 10° to 70°.

The combustion test was carried out on the Dual Analysis Cone Calorimeter (Fire Testing Technology Ltd., East Grinstead, West Sussex, UK) at an irradiance of 50 kW/m^2 according to ISO 5660-1 standard [40]. The materials were conditioned to equilibrium at 55% relative humidity and 23°C prior to testing. The dimensions of the samples were 100 × 100 mm. The thickness of the test specimens was 10 mm. These samples were horizontally arranged and protected by a stainless steel grid to prevent the samples from bending and expanding during the heating.

3. Results and Discussion

3.1. SEM Image Observations. Figure 1 shows typical surface SEM images of untreated wood and the treated wood. In Figure 1(a), smooth wood surface with some pits can be clearly observed from the SEM image. Fibrous wood structure is presented in the inset SEM image. In Figure 1(b), it is obvious that the wood surface is covered by a dense and uniform ZnO nanorod arrays coating without any presence of wood features compared with Figure 1(a). The inset SEM image indicates that well-aligned ZnO nanorods with a length of around 1 μm and a diameter of about 80 nm are perpendicularly located onto the wood surface. Moreover, these nanorods appear the same orientation directly on the wood surface and the surface of the nanorod is relatively glossy. In Figure 1(c), it seems that the wood surface is covered by a continuous TiO_2-decorated ZNAs film. From the inset image, it can be seen that the interspace between these nanorods is fully occupied by TiO_2 sol and the morphology of these well-aligned ZnO nanorods becomes an integrate construction connected by TiO_2 sol so that the ends of ZnO nanorods only projected slightly from the bulk surface. Simultaneously, the surface of these nanorods becomes much rougher than that of the bare ZnO nanorods shown in Figure 1(b). In Figure 1(d), the typical TEM image showed rod-like shape of the TiO_2-decorated ZnO nanorod peeled off from the treated wood sample by a strong ultrasonic treatment with 1800 W. The average size of the TiO_2 particles was about 25 nm. In the HRTEM image, the distances between the lattice planes of the ZnO part were measured to be 0.26 nm and 0.35 nm for TiO_2, respectively (Figure 1(d)). Additionally, the inset SAED pattern in top right corner of Figure 1(d) displays a polycrystalline diffraction with certain concentric rings, which was compatible with the XRD results shown in Figure 3(c).

3.2. EDXA Analysis. Figure 2 shows the elemental composition of wood specimens before and after hydrothermal treatment. In Figure 2(a), only oxygen, gold, and carbon elements can be detected from the spectra. The element of gold is from the coating layer used for SEM observation, and oxygen and carbon elements are from the wood substrate. In Figure 2(b), the new strong peaks of zinc element confirm that ZnO nanorods have been formed on the wood surface when the sample underwent hydrothermal procedure. In Figure 2(c), both peaks of zinc and titanium are synchronously presented. No other elements are detected which confirms that the surface of wood has been ornamented by a TiO_2-decorated ZnO nanorod arrays coating.

3.3. XRD Measurement. Figure 3 shows XRD patterns of untreated wood and treated wood. Apparently, compared with untreated wood (Figure 3(a)), the diffraction peaks at 15° and 22° belong to wood diffraction characteristic peaks in the treated woods [41–44]. The diffractogram of the untreated wood showed a high intensity crystalline peak I_{002} at 2θ = 22° and an amorphous peak with an intensity I_{am} at 2θ = 15° corresponding to the crystallographic plane (101). These characteristic peaks were attributed to cellulose based on the JCPDS data (03-0289). Some new strong diffraction peaks are observed in Figure 3(b), indicating the formation of new crystal structure on the wood surface. For ZNAs-coated wood specimen, all diffraction peaks could be well indexed to the wurtzite-type ZnO (JCPDS card number 36-1451). No excess peaks were detected, implying that only high purity ZnO nanostructure is formed after the hydrothermal reaction. In Figure 3(c), it can be distinctly found that new strong diffraction peaks are presented in comparison with Figure 3(a and b). All these diffraction peaks are readily indexed as wurtzite-type ZnO (JCPDS card number 36-1451) and anatase TiO_2 (JCPDS card number 21-1272). Simultaneously, in Figure 3(c), the diffraction peaks at 2θ = 8° were observed for treated wood by TiO_2-decorated ZnO nanorod arrays film, indicating a crystal structure with low crystallinity for TiO_2 nanoparticles. The observations reveal that TiO_2 nanoparticles would be polycrystalline. The diffractogram of the untreated wood showed a high intensity crystalline peak I_{002} at 2θ = 22° and an amorphous peak with an intensity I_{am} at 2θ = 15° corresponding to the crystallographic plane (101).

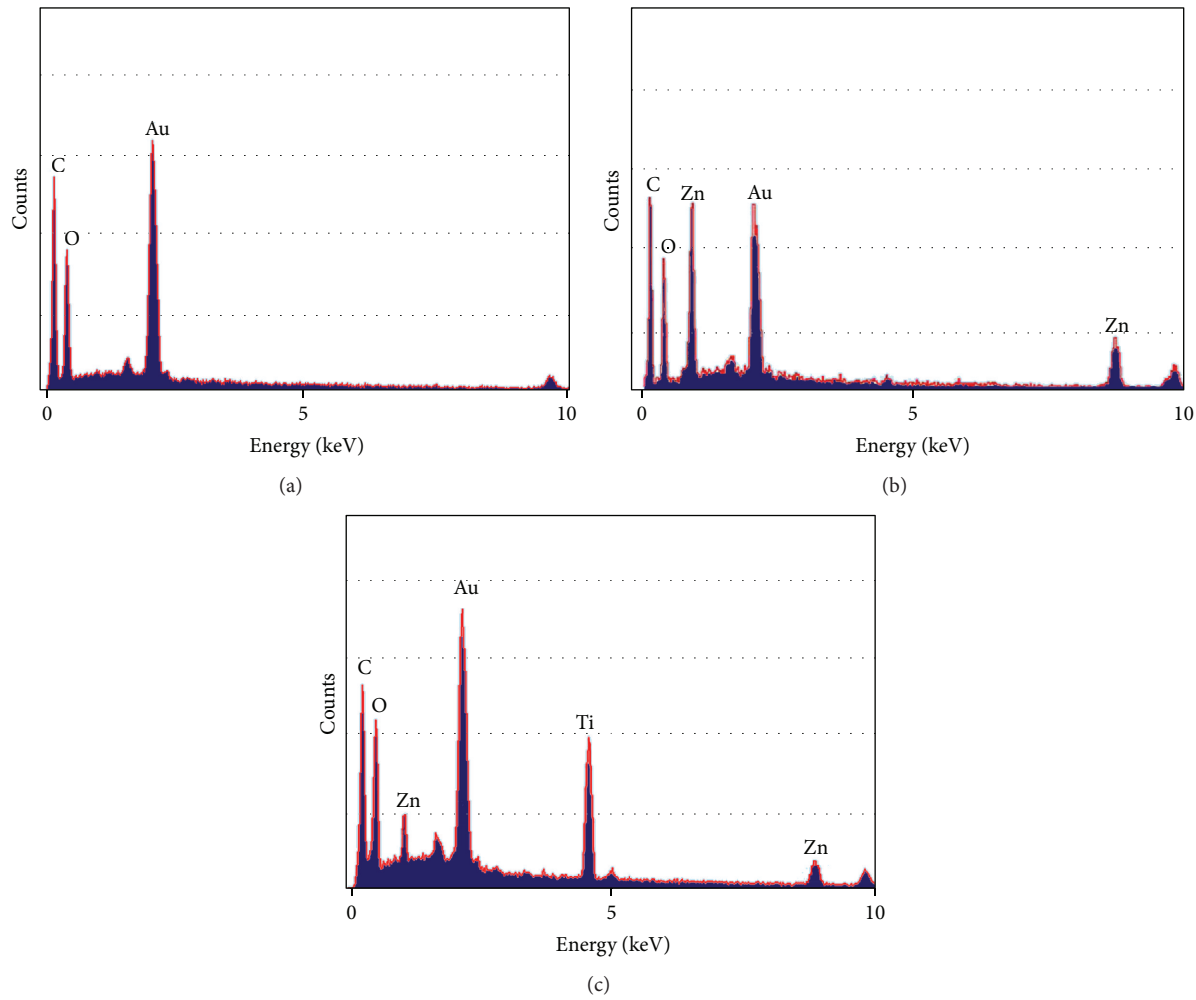

Figure 2: EDXA spectra of (a) untreated wood; (b) treated wood by ZnO nanorod arrays; and (c) treated wood by TiO_2-decorated ZnO nanorod arrays, respectively.

These characteristic peaks were attributed to cellulose based on the JCPDS data (03-0289).

In Figure 3(b and c), the (101) peak is not prominent in case of treated wood by ZnO nanorod arrays, whereas it is clear for TiO_2-decorated wood with ZnO nanorod arrays. This phenomenon could be ascribed to the increase of the crystallinity of cellulose after the hydrothermal treatment at a relatively high temperature (150°C), which was caused by the removal of partial hemicelluloses and lignin in the wood sample. XRD patterns suggest that a film of TiO_2-decorated ZnO nanorods has been structured on the wood surface.

3.4. Cone Calorimetry Testing

3.4.1. Time to Ignition (TTI). The TTI is one of the most important parameters to evaluate material fire resistance. The longer TTI means the better fire resistance. The TTI of the untreated and treated wood by a TiO_2-decorated ZNAs coating were 52 s and 35 s, respectively. It demonstrates that the TiO_2-decorated ZNAs coating has a negative capability for resisting fire ignition.

3.4.2. Heat Release Rate (HRR). The main parameter measured in the cone calorimeter is heat release rate (HRR). Figure 4 shows typical HRR curves of untreated wood and treated wood by a TiO_2-decorated ZNAs coating. For untreated wood, the first peak represents the wood beginning combustion before the char layer is formed. As the burning proceeds and a char layer is formed on the surface of wood, the HRR value decreases. The middle part is the pyrolysis of wood after the char layer is structured. The char layer makes a barrier coating for heat transfer into the material and the process of pyrolysis is slowed down. The heat release rate is accordingly reduced. The second peak indicates the increased rate of volatiles formation in the thin unburned part of specimen prior to the end of flame burning. The last part corresponds to the glowing combustion of the char residue at which volatiles had been already burned out. For wood burning, the most important key is how to decrease or restrain the heat release rate of the flaming burning of volatiles, which releases much higher heat rate than the combustion of char residue. The wood modified by TiO_2-decorated ZNAs thus has a strong influence on restraining the

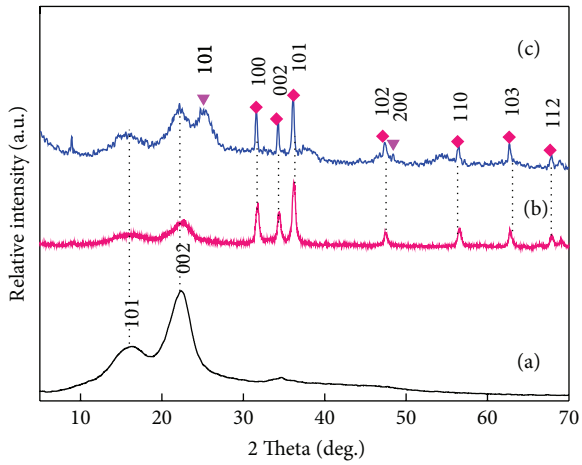

FIGURE 3: XRD patterns of (a) untreated wood; (b) treated wood by ZnO nanorod arrays; and (c) treated wood by TiO_2-decorated ZnO nanorod arrays, respectively. ▼ indicates the anatase phase of TiO_2 (JCPDS card number 21-1272); ◆ indicates the wurtzite phase of ZnO (JCPDS card number 36-1451).

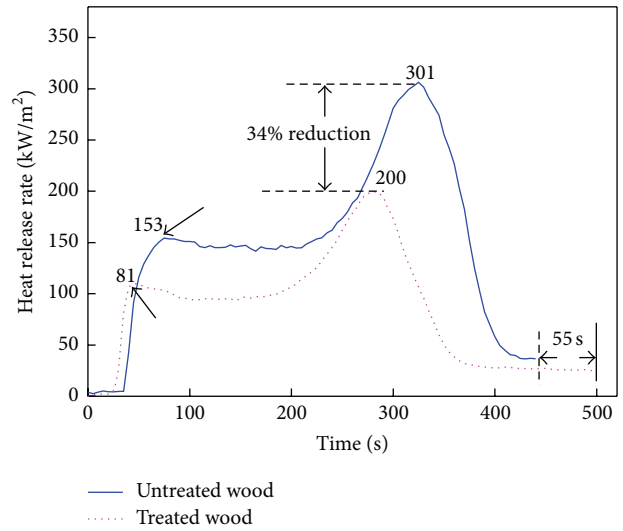

FIGURE 4: Heat release rate patterns of untreated wood and treated wood by a TiO_2-decorated ZnO nanorod arrays coating.

heat release rate throughout the wood burning duration. It clearly can be seen in Figure 4 that all the peak values of HRR are dramatically decreasing for the wood modified by TiO_2-decorated ZNAs. The first peak and second peak of the TiO_2-decorated ZNAs treated wood are all drastically reduced. The reduced values are 60.1% and 34%, respectively. Furthermore, the HRR curve seems much more moderate and relatively lower and the burning time was prolonged for 55 s, indicating the burning intensity and heat release are completely slowed and decreased. Apparently, the TiO_2-decorated ZNAs film has an outstanding capability for restraining the heat transfers to the wood substrate and thus reduces the heat release rates of the flammable volatiles from wood pyrolysis [45, 46].

3.4.3. Effective Heat of Combustion (EHC). The effective heat of combustion (EHC) measured in the cone calorimeter is mostly the flame burning condition which contributes to combustion of volatiles from material. It is obvious that the values of EHC shown in Figure 5 are lowered when the wood surface is covered by a TiO_2-decorated ZNAs coating because many water molecules absorbed on the surfaces of TiO_2 and ZnO nanorods can decrease the heat release [47–50]. Simultaneously, the continuous film of TiO_2-decorated ZNAs also can effectively hinder the combustion of volatiles. The reduction of EHC values of the treated wood specimens suggests that the TiO_2-decorated ZNAs films can effectively act as suppression for heat release and transfer and can be used for preparing antiflaming wood.

3.4.4. Total Heat Release (THR). The total heat release is defined as the total heat released by a material per unit area in a fire. Material with a high THR value will release more heat and, in general, the fire danger will be greater.

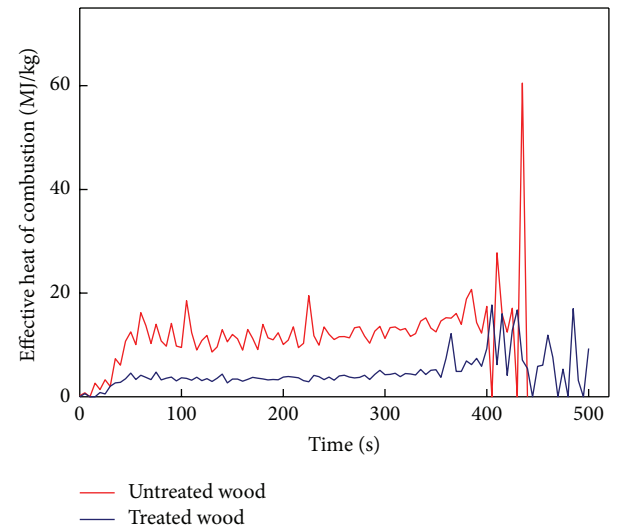

FIGURE 5: Effective heat of combustion patterns of untreated wood and treated wood by a TiO_2-decorated ZnO nanorod arrays coating.

Figure 6 shows the THR curves of the untreated, ZnO-treated wood, and treated wood, respectively. It is obvious that the THR curve of the treated wood is much lower than that of the untreated wood. The values of total heat release of the untreated, the ZnO-treated wood, and treated wood are 65.58 MJ/m^2, 54.06 MJ/m^2, and 42.13 MJ/m^2, respectively. The THR of the ZnO-treated wood decreased only by 17%, while the treated wood by ZNAs-decorated TiO_2 dramatically decreased by 35% in comparison with the untreated wood, which demonstrates that the TiO_2-decorated ZNAs have a positive influence on decreasing the total heat release.

3.4.5. Smoke Production Ratio (SPR) and Total Smoke Production (TSP). Wood smoke can decrease the view when wood is burning, which subsequently increases the harmfulness

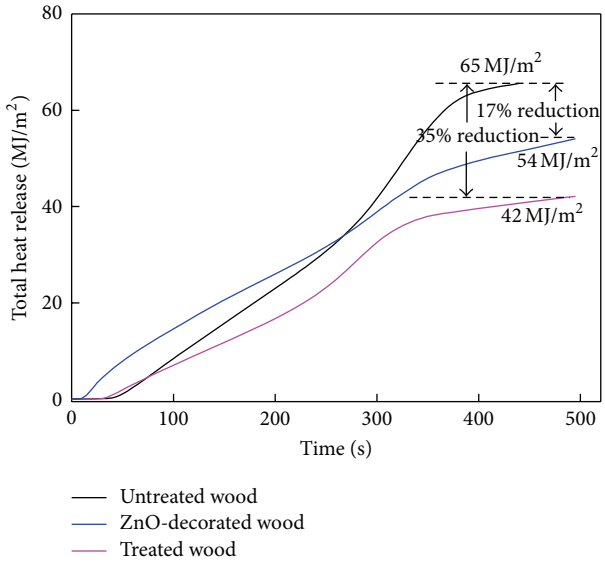

Figure 6: Total heat release patterns of untreated wood, the ZnO-treated wood, and the treated wood by a TiO_2-decorated ZnO nanorod arrays coating.

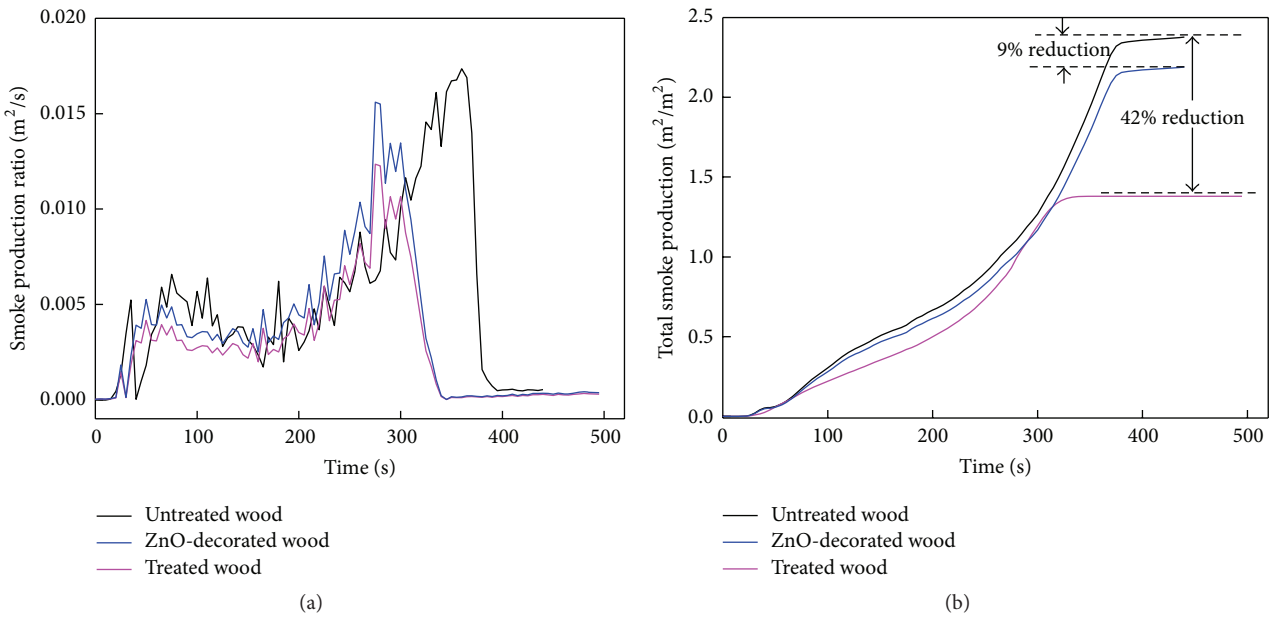

Figure 7: Smoke production rate and total smoke production patterns of the untreated wood, the ZnO-treated wood, and treated wood by a TiO_2-decorated ZnO nanorod arrays coating.

when wood burns. Reducing the smoke production is very useful in practice because it can increase the visuality and thus enhance the health safety for people. Compared with the untreated wood, the SPR and TSP of the ZnO-treated wood and the treated wood shown in Figure 7 are all decreased. The total TSP of the ZnO-treated wood was decreased by 9%. However, the total TSP was decreased by 42%. So, it can be concluded that the wood treated by a TiO_2-decorated ZNAs film is capable of blocking the wood smoke emission and production. It also indicates that TiO_2-decorated ZNAs can be applied as a substitute for smoke suppressants.

3.4.6. Production of CO and CO_2 (COY, CO2Y, COP, and CO2P). The main products of wood fire are carbon dioxide and water, but other toxic chemical compounds can also be released. The main released toxic material in wood fire is carbon monoxide (CO), which is the dominating toxic combustion product from burning wood. The yield of CO and CO_2 and the production of CO and CO_2 of the untreated and treated wood are measured and shown in Figures 8 and 9. For carbon monoxide, the COY and COP of the treated wood specimens are significantly reduced. At the beginning and middle of wood burning, the COY and COP are almost

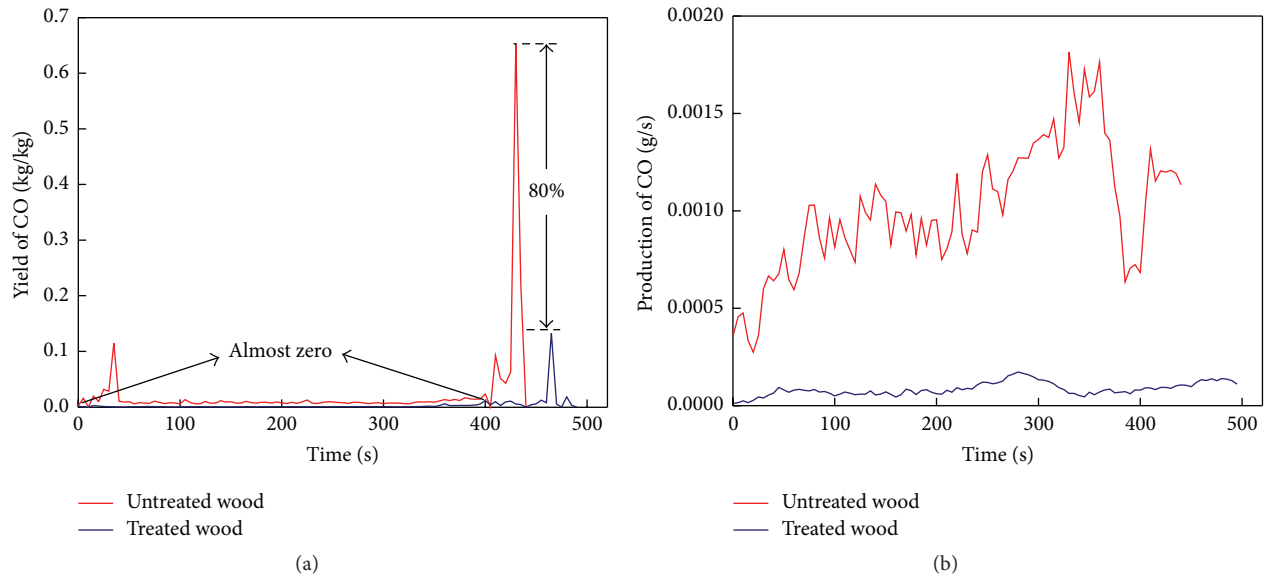

FIGURE 8: Yield of CO and production of CO patterns of untreated wood and treated wood by a TiO_2-decorated ZnO nanorod arrays coating.

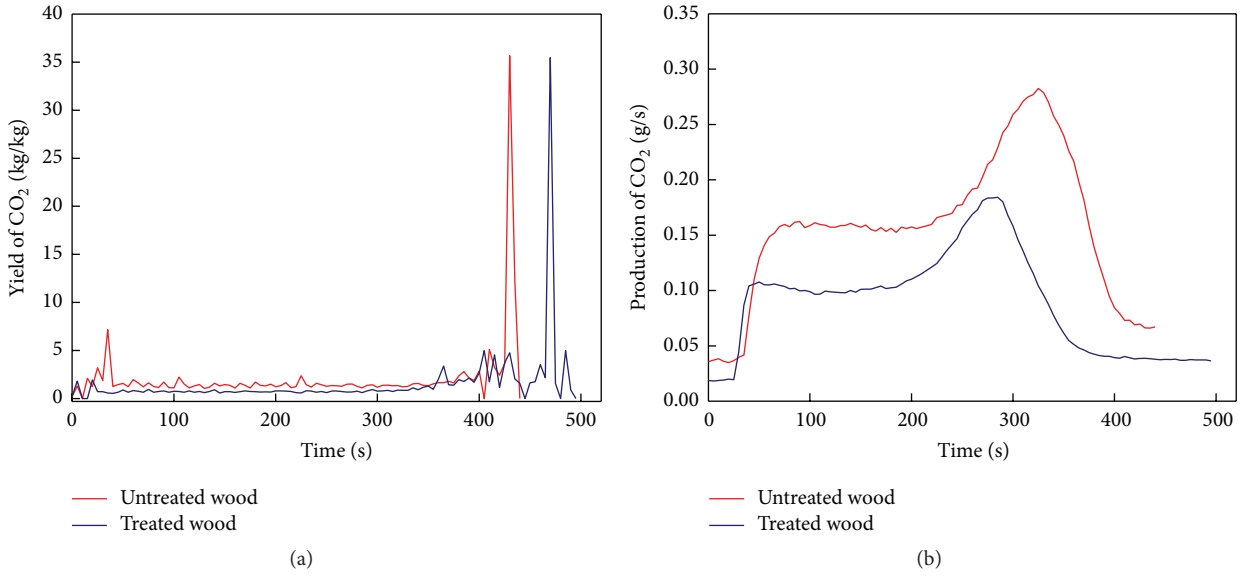

FIGURE 9: Yield of CO_2 and production of CO_2 patterns of untreated wood and treated wood by a TiO_2-decorated ZnO nanorod arrays coating.

zero. Till the end period, the carbon monoxide is decreased by 80%. For CO2Y and CO2P, there is no obvious decrease in spite of the somewhat reduction for CO2P. It can be concluded that the TiO_2-decorated ZNAs thin coating has a better performance for prohibiting the release of carbon monoxide than that of carbon dioxide.

3.4.7. Mass Loss (ML) and Mass Loss Rate (MLR). Figure 10 shows the ML and MLR curves of the untreated and treated wood. It can be seen that they have similar variation tendencies. The total mass loss value of the treated wood during the whole test was similar to that of the untreated wood, nearly 80% of the original weight. The residuum of the treated and untreated wood was about the same, which suggested that the retardant effect of the TiO_2-decroated ZNAs coating is not strong enough to stop burning until the flammable content of wood was burned out.

4. Conclusions

A TiO_2-decorated ZnO nanorod arrays film can functionally act as a fireproof material to change inflammable wood into nonflammable wood. Moreover, the thin inorganic nanomaterials film has an effective effect on restraining heat release and suppressing toxic smoke production. Modifying the wood by coating the surface with TiO_2-decorated ZnO

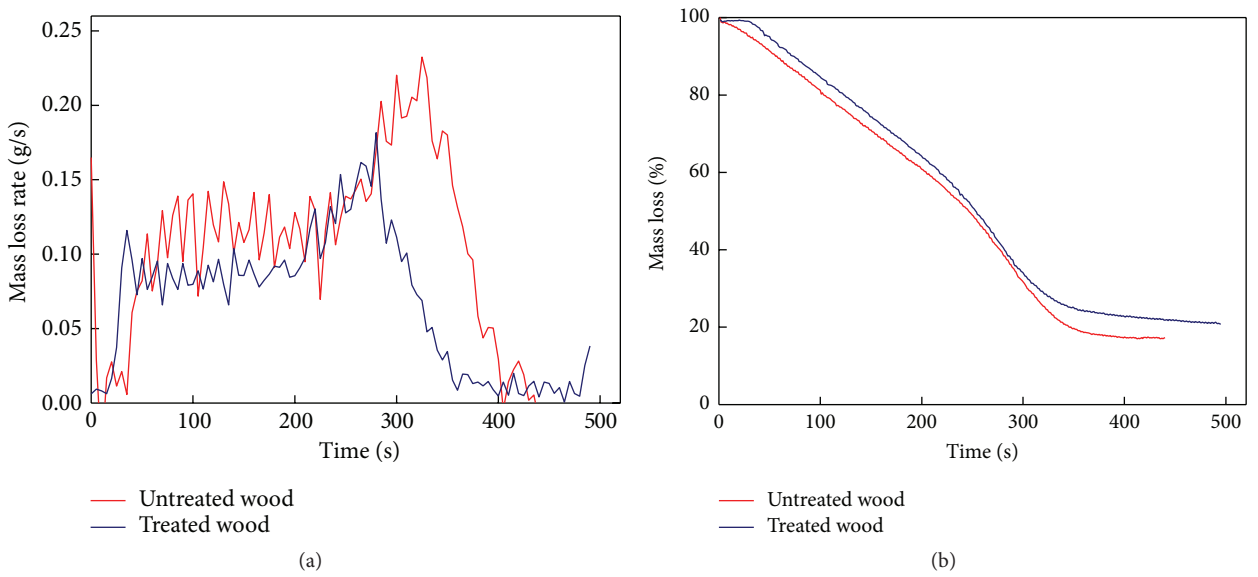

FIGURE 10: Mass loss rate and mass loss patterns of untreated wood and treated wood by a TiO_2-decorated ZnO nanorod arrays coating.

nanorod arrays provides a feasible pathway for fabrication of antiflaming wood.

Competing Interests

The authors declare that there are no competing interests regarding the publication of this manuscript.

Acknowledgments

This research was supported by Zhejiang Provincial Natural Science Foundation of China under Grant no. LY16C160006, the National Natural Science Foundation of China (31470586), and the Fund for Innovative Research Team of Forestry Engineering Discipline (101-206001000713).

References

[1] S. Kumar, "Chemical modification of wood," *Wood and Fiber Science*, vol. 26, pp. 270–280, 1994.

[2] V. Babrauskas, "Charring rate of wood as a tool for fire investigations," *Fire Safety Journal*, vol. 40, no. 6, pp. 528–554, 2005.

[3] J. Michael and P. Smith, "Satisfying consumers' 'Green' wants: an impetus for education," *Wood and Fiber Science*, vol. 26, no. 3, pp. 370–381, 1994.

[4] Q. Sun, H. Yu, Y. Liu, J. Li, Y. Cui, and Y. Lu, "Prolonging the combustion duration of wood by TiO_2 coating synthesized using cosolvent-controlled hydrothermal method," *Journal of Materials Science*, vol. 45, no. 24, pp. 6661–6667, 2010.

[5] Q. F. Sun, Y. Lu, H. M. Zhang et al., "Flame retardancy of wood coated by ZnO nanorod arrays via a hydrothermal method," *Materials Research Innovations*, vol. 16, no. 5, pp. 326–331, 2012.

[6] H. Mryafuji and S. Saka, "Fire-resisting properties in several TiO_2 wood-inorganic composites and their topochemistry," *Wood Science and Technology*, vol. 31, no. 6, pp. 449–455, 1997.

[7] M. Lewin, "Unsolved problems and unanswered questions in flame retardance of polymers," *Polymer Degradation and Stability*, vol. 88, no. 1, pp. 13–19, 2005.

[8] G. N. Inari, M. Pétrissans, A. Pétrissans, and P. Gérardin, "Elemental composition of wood as a potential marker to evaluate heat treatment intensity," *Polymer Degradation and Stability*, vol. 94, no. 3, pp. 365–368, 2009.

[9] M.-J. Chung, S.-S. Cheng, C.-J. Lee, and S.-T. Chang, "Novel environmentally-benign methods for green-colour protection of bamboo culms and leaves," *Polymer Degradation and Stability*, vol. 96, no. 4, pp. 541–546, 2011.

[10] S. Bourbigot and S. Duquesne, "Fire retardant polymers: recent developments and opportunities," *Journal of Materials Chemistry*, vol. 17, no. 22, pp. 2283–2300, 2007.

[11] J. Giancaspro, P. Balaguru, and R. Lyon, "Fire protection of flammable materials utilizing geopolymer," *SAMPE Journal*, vol. 40, no. 5, pp. 42–49, 2004.

[12] D. Katović, S. B. Vukušić, S. F. Grgac, J. Trajković, and V. Jirouš-Rajković, "Organophosphorus compounds for fire retardancy of wood," *Wood Research*, vol. 50, no. 2, pp. 59–66, 2005.

[13] F. A. Ximenes and P. D. Evans, "Protection of wood using oxy-aluminum compounds," *Forest Products Journal*, vol. 56, no. 11-12, pp. 116–122, 2006.

[14] S. Hamdani, C. Longuet, D. Perrin, J.-M. Lopez-Cuesta, and F. Ganachaud, "Flame retardancy of silicone-based materials," *Polymer Degradation and Stability*, vol. 94, no. 4, pp. 465–495, 2009.

[15] S. Hribernik, M. S. Smole, K. S. Kleinschek, M. Bele, J. Jamnik, and M. Gaberscek, "Flame retardant activity of SiO_2-coated regenerated cellulose fibres," *Polymer Degradation and Stability*, vol. 92, no. 11, pp. 1957–1965, 2007.

[16] E. Baysal, M. Altinok, M. Colak, S. K. Ozaki, and H. Toker, "Fire resistance of Douglas fir (Pseudotsuga menzieesi) treated with borates and natural extractives," *Bioresource Technology*, vol. 98, no. 5, pp. 1101–1105, 2007.

[17] M. Hagen, J. Hereid, M. A. Delichatsios, J. Zhang, and D. Bakirtzis, "Flammability assessment of fire-retarded Nordic

Spruce wood using thermogravimetric analyses and cone calorimetry," *Fire Safety Journal*, vol. 44, no. 8, pp. 1053–1066, 2009.

[18] T. Harada, "Progress toward the development of fire-resistant wooden structures in Japan," *Mokuzai Gakkaishi*, vol. 55, no. 1, pp. 1–9, 2009.

[19] S. Pavlidou and C. D. Papaspyrides, "A review on polymer-layered silicate nanocomposites," *Progress in Polymer Science*, vol. 33, no. 12, pp. 1119–1198, 2008.

[20] G. Beyer, "Nanocomposites offer new way forward for flame retardants," *Plastics, Additives and Compounding*, vol. 7, no. 5, pp. 32–35, 2005.

[21] H. Fischer, "Polymer nanocomposites: from fundamental research to specific applications," *Materials Science and Engineering C*, vol. 23, no. 6-8, pp. 763–772, 2003.

[22] M. Saxena, R. K. Morchhale, P. Asokan, and B. K. Prasad, "Plant fiber—industrial waste reinforced polymer composites as a potential wood substitute material," *Journal of Composite Materials*, vol. 42, no. 4, pp. 367–384, 2008.

[23] X.-Y. Ma and W.-D. Zhang, "Effects of flower-like ZnO nanowhiskers on the mechanical, thermal and antibacterial properties of waterborne polyurethane," *Polymer Degradation and Stability*, vol. 94, no. 7, pp. 1103–1109, 2009.

[24] D. Yang, S. Sarina, H. Zhu et al., "Capture of radioactive cesium and iodide ions from water by using titanate nanofibers and nanotubes," *Angewandte Chemie—International Edition*, vol. 50, no. 45, pp. 10594–10598, 2011.

[25] D. S. Kim and S.-Y. Kwak, "The hydrothermal synthesis of mesoporous TiO_2 with high crystallinity, thermal stability, large surface area, and enhanced photocatalytic activity," *Applied Catalysis A: General*, vol. 323, pp. 110–118, 2007.

[26] X. Chen and S. S. Mao, "Titanium dioxide nanomaterials: synthesis, properties, modifications, and applications," *Chemical Reviews*, vol. 107, no. 7, pp. 2891–2959, 2007.

[27] C. F. Klingshirn, "ZnO: material, physics and applications," *ChemPhysChem*, vol. 8, no. 6, pp. 782–803, 2007.

[28] Ü. Özgür, Y. I. Alivov, C. Liu et al., "A comprehensive review of ZnO materials and devices," *Journal of Applied Physics*, vol. 98, no. 4, Article ID 041301, 103 pages, 2005.

[29] V. Devi, M. Kumar, R. Kumar, and B. C. Joshi, "Effect of substrate temperature and oxygen partial pressure on structural and optical properties of Mg doped ZnO thin films," *Ceramics International*, vol. 41, no. 5, pp. 6269–6273, 2015.

[30] V. Devi, M. Kumar, R. Kumar, A. Singh, and B. C. Joshi, "Band offset measurements in $Zn_{1-x}Sb_xO$/ZnO hetero-junction," *Journal of Physics D: Applied Physics*, vol. 48, no. 33, Article ID 335103, 2015.

[31] M. S. Roy, P. Balraju, M. Kumar, and G. D. Sharma, "Dye-sensitized solar cell based on Rose Bengal dye and nanocrystalline TiO_2," *Solar Energy Materials and Solar Cells*, vol. 92, no. 8, pp. 909–913, 2008.

[32] M. L. Singla, M. Shafeeq M, and M. Kumar, "Optical characterization of ZnO nanoparticles capped with various surfactants," *Journal of Luminescence*, vol. 129, no. 5, pp. 434–438, 2009.

[33] B. Mahltig, C. Swaboda, A. Roessler, and H. Bottcher, "Functionalising wood by nanosol application," *Journal of Materials Chemistry*, vol. 18, pp. 3180–3192, 2008.

[34] H. Miyafuji and S. Saka, "Wood-inorganic composites prepared by the sol-gel process .5. Fire-resisting properties of the SiO2-P2O5-B2O3 wood-inorganic composites," *Mokuzai Gakkaishi*, vol. 42, no. 1, pp. 74–80, 1996.

[35] V. Blanchard and P. Blanchet, "Color stability for wood products during use: effects of inorganic nanoparticles," *BioResources*, vol. 6, no. 2, pp. 1219–1229, 2011.

[36] C. A. Clausen, F. Green III, and S. N. Kartal, "Weatherability and leach resistance of wood impregnated with nano-zinc oxide," *Nanoscale Research Letters*, vol. 5, no. 9, pp. 1464–1467, 2010.

[37] S. L. Wang, J. Y. Shi, C. Y. Liu, C. Xie, and C. Y. Wang, "Fabrication of a superhydrophobic surface on a wood substrate," *Applied Surface Science*, vol. 257, no. 22, pp. 9362–9365, 2011.

[38] F. Weichelt, R. Emmler, R. Flyunt, E. Beyer, M. R. Buchmeiser, and M. Beyer, "ZnO-based UV nanocomposites for wood coatings in outdoor applications," *Macromolecular Materials and Engineering*, vol. 295, no. 2, pp. 130–136, 2010.

[39] M. A. Tshabalala and J. E. Gangstad, "Accelerated weathering of wood surfaces coated with multifunctional alkoxysilanes by sol-gel deposition," *Journal of Coatings Technology*, vol. 75, no. 943, pp. 37–43, 2003.

[40] O. Grexa and H. Lübke, "Flammability parameters of wood tested on a cone calorimeter," *Polymer Degradation and Stability*, vol. 74, no. 3, pp. 427–432, 2001.

[41] M. Kumar, R. C. Gupta, and T. Sharma, "X-ray diffraction studies of *Acacia* and *Eucalyptus* wood chars," *Journal of Materials Science*, vol. 28, no. 3, pp. 805–810, 1993.

[42] T. Paakkari and R. Serimaa, "A study of the structure of wood cells by x-ray diffraction," *Wood Science and Technology*, vol. 18, no. 2, pp. 79–85, 1984.

[43] M.-P. Sarén and R. Serimaa, "Determination of microfibril angle distribution by X-ray diffraction," *Wood Science and Technology*, vol. 40, no. 6, pp. 445–460, 2006.

[44] M. Kalliat, C. Y. Kwak, P. W. Schmidt, B. E. Cutter, and E. A. McGinnes, "Small angle X-ray scattering measurement of porosity in wood following pyrolysis," *Wood Science and Technology*, vol. 17, no. 4, pp. 241–257, 1983.

[45] L. J. Goff, "Investigation of polymeric materials using the cone calorimeter," *Polymer Engineering and Science*, vol. 33, no. 8, pp. 497–500, 1993.

[46] N. M. Stark, R. H. White, and C. M. Clemons, "Heat release rate of wood-plastic composites," *SAMPE Journal*, vol. 33, no. 5, pp. 26–31, 1997.

[47] L. Jing, Z. Xu, X. Sun, J. Shang, and W. Cai, "The surface properties and photocatalytic activities of ZnO ultrafine particles," *Applied Surface Science*, vol. 180, no. 3-4, pp. 308–314, 2001.

[48] C. Wöll, "The chemistry and physics of zinc oxide surfaces," *Progress in Surface Science*, vol. 82, no. 2-3, pp. 55–120, 2007.

[49] U. Diebold, "The surface science of titanium dioxide," *Surface Science Reports*, vol. 48, no. 5–8, pp. 53–229, 2003.

[50] T. L. Thompson and J. T. Yates Jr., "Surface science studies of the photoactivation of TiO_2—new photochemical processes," *Chemical Reviews*, vol. 106, no. 10, pp. 4428–4453, 2006.